Take a deep dive into the business of transplantation!

2021 Digital Kidney & Liver Transplant Financial Bootcamp

Access Online!

Self-paced: access at your convenience

Register at ASTS.org/bootcamps

ASTS
American Society of Transplant Surgeons®

American Journal of Transplantation 2016; 16: 2016–2029
Wiley Periodicals Inc.

doi: 10.1111/ajt.13704

Cell Therapy for Parkinson's Disease: A Translational Approach to Assess the Role of Local and Systemic Immunosuppression

R. Aron Badin[1,*], M. Vadori[3], B. Vanhove[4,5], V. Nerriere-Daguin[4], P. Naveilhan[6], I. Neveu[6], C. Jan[1], X. Lévèque[4], E. Venturi[7], P. Mermillod[7], N. Van Camp[1], F. Dollé[2], M. Guillermier[1], L. Denaro[8], R. Manara[8], V. Citton[8], P. Simioni[8], P. Zampieri[8], D. D'avella[8], D. Rubello[9], F. Fante[3], M. Boldrin[3], G. M. De Benedictis[10], L. Cavicchioli[11], D. Sgarabotto[12], M. Plebani[13], A. L. Stefani[14], P. Brachet[4], G. Blancho[4,5], J. P. Soulillou[4], P. Hantraye[1] and E. Cozzi[3,15]

[1]*MIRCen, CEA UMR 9199, Fontenay-aux-Roses, France*
[2]*CEA, I²BM, Service Hospitalier Frédéric Joliot, Orsay, France*
[3]*CORIT (Consortium for Research in Organ Transplantation), Padua, Italy*
[4]*Institut National de la Santé et de la Recherche Médicale UMR1064, Nantes, France*
[5]*CHU de Nantes, Institut de Transplantation Urologie Néphrologie, Université de Nantes, Nantes, France*
[6]*Institut National de la Santé et de la Recherche Médicale UMR913, Nantes, France*
[7]*INRA Physio Reproduction Femelle CR de Tours, Nouzilly, France*
[8]*Neurosciences, University of Padua, Padua, Italy*
[9]*Nuclear Medicine, S. Maria della Misericordia Hospital, Rovigo, Italy*
[10]*Department of Animal Medicine, Production and Health, University of Padua, Legnaro, Italy*
[11]*Department of Comparative Biomedicine and Food Science, University of Padua, Legnaro, Italy*
[12]*Transplant Infectious Disease Unit, Padua University Hospital, Padua, Italy*
[13]*Department of Laboratory Medicine, Padua University Hospital, Padua, Italy*
[14]*Istituto Zooprofilattico Sperimentale delle Venezie, Legnaro, Italy*
[15]*Transplant Immunology Unit, Padua University Hospital, Padua, Italy*
**Corresponding author: Romina Aron Badin, romina.aron-badin@cea.fr*

Neural transplantation is a promising therapeutic approach for neurodegenerative diseases; however, many patients receiving intracerebral fetal allografts exhibit signs of immunization to donor antigens that could compromise the graft. In this context, we intracerebrally transplanted mesencephalic pig xenografts into primates to identify a suitable strategy to enable long-term cell survival, maturation, and differentiation. Parkinsonian primates received WT or CTLA4-Ig transgenic porcine xenografts and different durations of peripheral immunosuppression to test whether systemic plus graft-mediated local immunosuppression might avoid rejection. A striking recovery of spontaneous locomotion was observed in primates receiving systemic plus local immunosuppression for 6 mo. Recovery was associated with restoration of dopaminergic activity detected both by positron emission tomography imaging and histological examination. Local infiltration by T cells and CD80/86+ microglial cells expressing indoleamine 2,3-dioxigenase were observed only in CTLA4-Ig recipients. Results suggest that in this primate neurotransplantation model, peripheral immunosuppression is indispensable to achieve the long-term survival of porcine neuronal xenografts that is required to study the beneficial immunomodulatory effect of local blockade of T cell costimulation.

Abbreviations: (^{18}F)DPA-714, *N,N*-diethyl-2-(2-[4-2-(^{18}F) fluoroethoxy]phenyl-5,7-dimethylpyrazolo[1,5-a]pyrimidin-3-yl)acetamide; (^{18}F)F-L-DOPA, 6-(18F)fluoro-3,4-dihydroxy-L-phenylalanine; CSF, cerebrospinal fluid; d, days; FITC, fluorescein isothiocyanate; G, group; IS, immunosuppression; Ki, inhibition constant; MFI, median fluorescence intensity; MPTP, 1-methyl-4-phenyl-1,2,3,6-tetrahydropyridine; mo, months; MRI, magnetic resonance imaging; NF70, neurofilament 70; NS, not significant; PAEC, porcine aortic endothelial cells; PD, Parkinson's disease; PET, positron emission tomography; w, weeks

Received 22 June 2015, revised 29 November 2015 and accepted for publication 22 December 2015

Introduction

Cell-based regenerative therapies have been tested in Parkinson's disease (PD) and Huntington's disease with various outcomes including both significant long-lasting recovery and serious adverse effects (1–10). The variability in outcomes has been linked to patient selection and tissue preparation, poor cell survival, host pathology spreading to the grafted cells and graft immunogenicity in the long term even after allotransplantation (1,2,11). In

particular, the immune system's contribution to the progression of the pathology from the host to the graft and to the inflammatory reaction at the graft–host interface could severely compromise the long-term survival and functionality of the transplanted cells (3–7). The brain has been considered an immune-privileged site for decades, and the roles of T cell–mediated graft rejection and of the humoral immune response have been largely underestimated in clinical allografting trials to date. In the xenograft literature, however, several studies have suggested that porcine cells transplanted into the brain of rodents (12–16), nonhuman primates (17) and patients (18) activate the host immune system through peripheral and local presentation of xenoantigens to reactive T cells. Activated microglia and CD8+ T cells have been found to infiltrate porcine neural xenografts, even under cyclosporine immunosuppression (19). Antibody-mediated depletion of CD4+ cells in xenografted rats suggests that T helper lymphocytes, in particular Th1, play a pivotal role in neural xenograft rejection (13,20–22).

This study used the pig-to-primate xenotransplantation model to evaluate the efficacy of adding a local immunosuppressive treatment to systemic immunosuppression to extend the survival of transplanted cells. Our hypothesis is that CTLA4-Ig, a well-characterized modulator of T cell activation, may decrease the antigraft humoral immune response (23). Genetically engineered pig embryos expressing high levels of neuronal CTLA4-Ig were used to explore the possible synergistic effect of intragraft expression of a costimulation blocker and a peripheral immunosuppressive regimen in preventing local xenogeneic B and T cell activation in primates (24). The two primary readouts of graft differentiation and functionality were the capacity of pig neuroblasts to differentiate into mature dopaminergic neurons bearing amino acid decarboxylase activity and their ability to correct for akinesia in a primate model of PD.

Materials and Methods

Animals and housing

All experiments were conducted according to European (EU Directive 86/609/EEC), French (authorization A 92-032-02) and Italian (authorizations 151/2007-C and 30/2011-C) regulations.

Nineteen (3 male, 16 female) *Macaca fascicularis* (Sicombrec, Makati, Philippines) with a mean age of 7 ± 2 years and a mean weight of 3.7 ± 1 kg were housed under standard environmental conditions (12-h light–dark cycle, 22 ± 1°C, 50% humidity) with free access to food and water.

Pig breeding was performed at the Institut National de Recherche Agronomique in compliance with institutional guidelines. Donor females were Large White hyperprolific pubertal gilts. Estrus was synchronized, as described previously (25, 26), and 3 days later, female pigs were surgically inseminated into the fallopian tubes with cryopreserved sperm from WT or NSE-CTLA4-Ig+/+ boars expressing CTLA4-Ig in neurons under the transcriptional control of the neuron-specific enolase promoter (24).

Experimental design

The workflow of the experiments is presented in Figure 1.

Parkinsonism was induced by 7-day cycles of intramuscular injections of 0.25 mg/kg of 1-methyl-4-phenyl-1,2,3,6-tetrahydropyridine (MPTP; Sigma-Aldrich, St. Louis, MO) until a significant reduction (≥80%) in spontaneous locomotor activity was measured, as described previously (27). Five 40-min baseline videos were acquired to quantify the total distance moved in centimeters using Ethovision software (Noldus, Wageningen, The Netherlands) (27–29). Characterization of the MPTP model is included as supplementary material (Figure S1). Primates were filmed weekly during MPTP and biweekly following transplantation.

Prior to surgery, primates were sedated with ketamine (6 mg/kg) and buprenorphine (0.01 mg/kg), induced with propofol (2.5 mg/kg) and midazolam (0.3 mg/kg), and maintained with sevoflurane (1.9%). Temperature was maintained at 37°C, and oxygen saturation as measured by pulse oximetry, end-tidal CO_2, noninvasive blood pressure, and respiratory and cardiac rates were monitored remotely. Small solid pieces of ventral mesencephalon (<1 × 1 × 1 mm) dissected from 10 ± 2 CTLA4-Ig

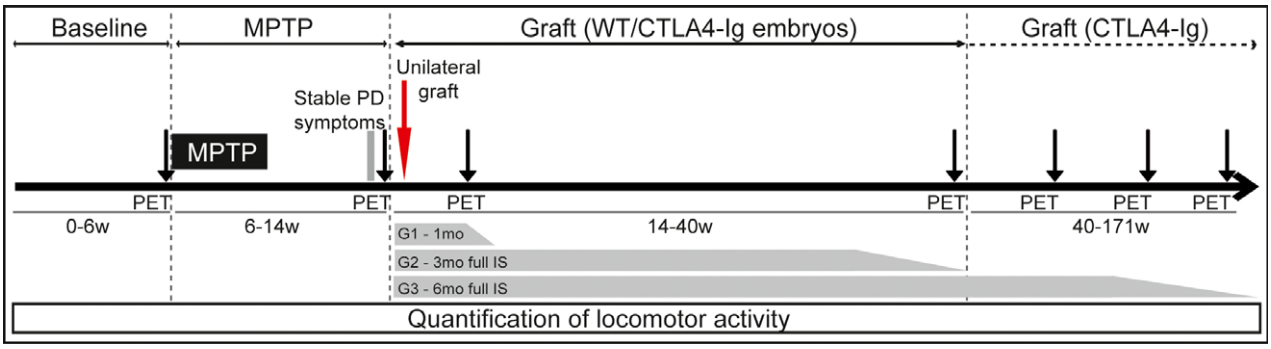

Figure 1: Schematic representation of the experimental design and pharmacological treatment protocols. General experimental plan showing its duration (in weeks) and phases: baseline, MPTP intoxication, and follow-up after transplantation (Graft) with WT or CTLA4-Ig transgenic pig embryos. Quantification of locomotor activity was performed periodically throughout the experiment, and PET time points are indicated by vertical arrows. The duration of follow-up after transplantation and of the full immunosuppressive regimen for each group are shown. A subset of two primates in group 3 that survived >6 mo is indicated by the top dashed arrow. G, group; IS, immunosuppression; MPTP, 1-methyl-4-phenyl-1,2,3,6-tetrahydropyridine; PET, positron emission tomography; w, weeks; mo, months.

transgenic or WT pig embryos were stereotactically injected into the left putamen (2 × 25 μL). Postoperative analgesia consisted of buprenorphine (0.01 mg/kg) for 3 days.

Animals were grouped according to three durations of oral immunosuppressive therapy (Table S1) consisting of cyclosporin A, sodium mycophenolate mofetil and prednisone at doses recommended for this species (Table S2) (30). Periodic blood sampling was performed to monitor drug levels, general biochemistry and hematology.

Imaging studies

Anatomical magnetic resonance imaging was performed under general anesthesia to precisely determine the regions of interest for positron emission tomography (PET) analysis and the surgical implantation coordinates. PET scans were acquired under general anesthesia using either 6-(18F)fluoro-3,4-dihydroxy-L-phenylalanine ([18F]F-L-DOPA) or N,N-diethyl-2-(2-[4-(2-(18F)fluoroethoxy]phenyl)-5,7-dimethylpyrazolo[1,5-a]pyrimidin-3-yl)acetamide ([18F]DPA-714) (31). Details of the acquisition methods and data analysis are included as supplementary material.

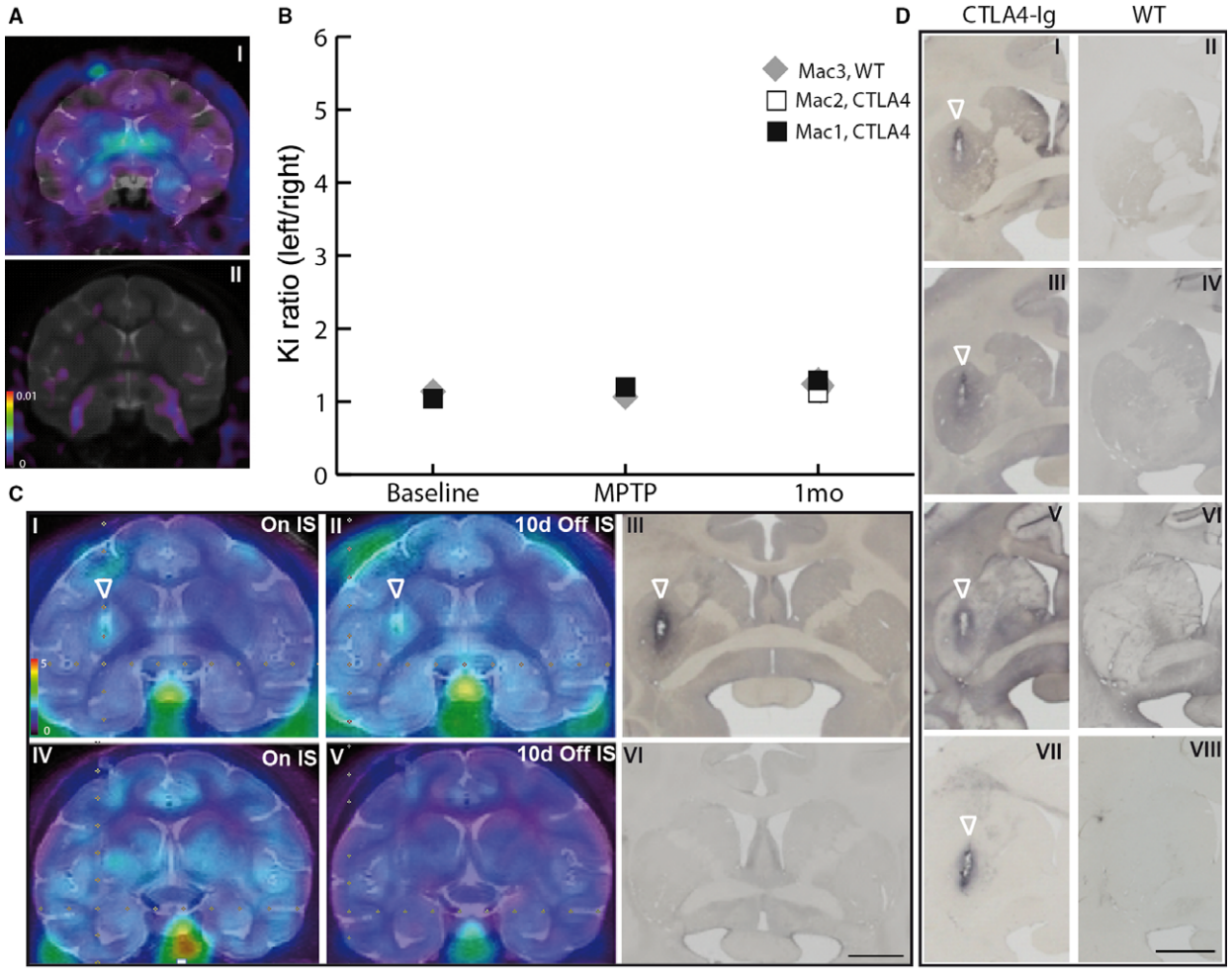

Figure 2: Effect of 1 mo of full peripheral immunosuppressive therapy following porcine embryonic grafts in parkinsonian primates. (A) Representative (18F)F-L-DOPA Ki PET coronal images overlapped with anatomical MRI images at MPTP (I) and 1 mo after grafting under full systemic immunosuppressive therapy (II). (B) Ratio of left (grafted) and right (ungrafted) putaminal Ki values showing the quantification of PET (18F)F-L-DOPA radiotracer at baseline, at MPTP, and at 1 mo after grafting in all primates in group 1. No differences in (18F)F-L-DOPA uptake were observed between animals or between the different time points measured. (C) (18F)DPA-714 standard uptake value PET coronal images overlapped with anatomical MRI images showing neuroinflammation at 1 mo after grafting under full systemic immunosuppressive therapy (I, IV) and at 10 days after complete withdrawal of systemic immunosuppressive therapy (II, V) following transplantation of CTLA4-Ig (I, II, III) or WT (IV, V, VI) pig embryonic cells. The PET images and the corresponding Iba1 immunohistochemistry (III, VI) suggest ongoing rejection of the CTLA4-Ig transplant. (D) Histological analysis of CTLA4-Ig– and WT-grafted parkinsonian primates showing coronal sections at the anterior commissure level stained for TH (I, II), NF70 (III, IV), GFAP (V, VI), and CD68 (VII, VIII), showing the presence of porcine (NF70) differentiated (TH) cells and active glial cells only in the CTLA4-Ig recipient. Scale bars = 500 μm. (18F)DPA-714, *N,N*-diethyl-2-(2-(4-2-(18F)fluoroethoxy)phenyl)-5,7-dimethylpyrazolo(1,5-a)pyrimidin-3-yl)acetamide; (18F)F-L-DOPA, 6-(18F) fluoro-3,4-dihydroxy-L-phenylalanine; d, days; mo, months; IS, immunosuppression; Ki, inhibition constant; MPTP, 1-methyl-4-phenyl-1,2,3,6-tetrahydropyridine; MRI, magnetic resonance imaging; NF70, neurofilament 70; PET, positron emission tomography.

Postmortem studies

After transcardial perfusion with 4% paraformaldehyde, brains were extracted and processed. Sections were incubated with primary antibodies against TH (ImmunoStar, Hudson, WI), GFAP (DakoCytomation, Glostrup, Denmark), NeuN (Millipore, Darmstadt, Germany), neurofilament 70 (NF70; Millipore) or Iba1 (Wako, Tokyo, Japan). Graft cellular infiltrate characterization was performed using rabbit antihuman CD3 (Dako), CD8 (Beckman-Coulter, Brea, CA), CD20 (Dako), CD80 (Fujirebio, Ghent, Belgium), Foxp3 (eBiosciences, San Diego) and IDO (Adipogen, Epalinges, Switzerland). Sections were then incubated with either Alexa 568–labeled goat antimouse IgG (Invitrogen, Carlsbad, CA) or fluorescein isothiocyanate (FITC)–labeled goat antirabbit IgG (Jackson ImmunoResearch, West Grove, PA) and analyzed using Axioskop 2 plus microscope (Zeiss, Oberkochen, Germany) and/or confocal Nikon A1, Software NIS Element (Nikon, Tokyo, Japan).

Antipig antibodies were measured in serum and cerebrospinal fluid (CSF) by flow cytometry crossmatch using pig embryonic neural cells or porcine aortic endothelial cells, as described previously (32). Briefly, samples were incubated (30 min, 4°C) with 200 000 pig cells and goat antimonkey IgG conjugated to FITC (AbD Serotec, Oxford, U.K.). Median fluorescence intensity was recorded using an LSR-II flow cytometer and analyzed by DIVA (Becton-Dickinson, Franklin Lakes, NJ) and FlowJo software (FlowJo LLC, Ashland, OR).

Statistical analysis

For the quantification of locomotor activity, each animal was compared with itself at baseline, at MPTP and at all time points after transplantation. Behavioral, histological and PET data were analyzed using the Student t-test or one-way analysis of variance followed by the Fisher least significant difference post hoc test. Data are expressed as mean plus or minus standard error of the mean.

Results

One-month systemic immunosuppressive therapy

In group 1 (n = 3), parkinsonian primates were grafted with CTLA4-Ig (n = 2) or WT (n = 1) porcine neuroblasts under full systemic immunosuppressive therapy for 30 days and were completely withdrawn from all medication for 12 days before euthanasia.

PET imaging with (18F)F-L-DOPA showed no differences in dopamine metabolism in WT or transgenic graft recipients (not significant [NS], p = 0.7) at 1 mo after grafting (still under systemic immunosuppression) compared with MPTP. No primate showed differences between grafted and ungrafted hemispheres at 1 mo after transplantation (NS, p = 0.98) (Figures 2AI, II and B).

PET scans with (18F)DPA-714 that were obtained 1 mo after grafting and at 6 days (data not shown) and 10 days following immunosuppression withdrawal (Figures 2CI, II, IV, V) showed a positive unilateral signal in one CTLA4-Ig–grafted primate before and after systemic immunosuppression withdrawal (Figures 2CI, II). This signal correlated with marked Iba1 immunostaining in the grafted area that was suggestive of neuroinflammation that was not observed in the WT graft recipient (Figures 2CIII, VI).

A few TH-positive (Figure 2DI) and NF70-positive porcine fibers (Figure 2DIII) were observed in the striatum of CTLA4-Ig graft recipients only (Figures 2DII, IV). GFAP and CD68 were also present in the grafted area, suggesting a mild inflammatory response to the xenograft in CTLA4-Ig recipients 12 days after systemic immunosuppressive therapy withdrawal (Figures 2DV, VII).

Three-month systemic immunosuppressive therapy

In group 2, 10 parkinsonian primates were kept under full immunosuppression for 3 mo following transplantation with CTLA4-Ig (n = 5) or WT (n = 5) porcine neuroblasts and were then withdrawn gradually.

PET scans with (18F)DPA-714 at 3 mo after injection showed no neuroinflammatory reaction in a subset of four primates, two WT and two CTLA4-Ig recipients (Figures 3AI, II). PET scans with (18F)F-L-DOPA that were performed at baseline, after MPTP intoxication and at 6 mo after grafting in all animals showed a positive (18F)F-L-DOPA signal in the grafted striatum in only one CTLA4-Ig and one WT recipient (Figures 3AIII, IV). The influx constant (Ki) ratio between MPTP and 6 mo after transplantation showed no significant changes in (18F)F-L-DOPA signal in the grafted and ungrafted hemispheres in all other WT- and CTLA4-Ig–grafted primates over time (NS, p = 0.6) (Figure 3B).

The fold increase in locomotor recovery from MPTP values for each primate following transplantation showed no significant differences between WT- and CTLA4-Ig–grafted primates (NS, p = 0.9) (Figure 3C). At peak recovery (118.8 ± 17.6 days after grafting), the mean fold increase was 2.4 ± 0.6 in CTLA4-Ig recipients and 2.1 ± 0.3 in WT recipients. Similarly, no differences were seen at 6 mo after transplantation between WT (1.6 ± 0.1) and CTLA4-Ig (1.3 ± 0.1) recipients; however, 60% of all primates showed at least a 1.5-fold increase in locomotor activity at the end point compared with MPTP values.

Histological examination at 6 mo after transplantation explained the variability of *in vivo* outcomes. Of 10 primates, only one CTLA4-Ig and one WT recipient showed a graft that was associated with a positive (18F)F-L-DOPA signal and that stained strongly positive for TH, NF70, CTLA4-Ig and GFAP (Figures 3DI, II, III, IV) and moderately for Iba1 and CD68 (Figures 3DV, VI). All other primate brains stained mildly for CD68, Iba1 and GFAP at this time point, suggesting an inflammatory signature (data not shown).

Six-month systemic immunosuppressive therapy

Six-month survival: Because of the variable results of group 2 and to evaluate the effect of mature grafts expressing adequate levels of CTLA4-Ig, the duration of full immunosuppression was doubled. The six

Figure 3: Effect of 3 mo of full systemic immunosuppressive therapy following porcine embryonic cell grafts in parkinsonian primates. (A) (18F)DPA-714 standard uptake value (I, II) and (18F)F-L-DOPA Ki (III, IV) PET coronal images overlapped with anatomical magnetic resonance imaging in CTLA4-Ig–grafted (top row) and WT-grafted (lower row) parkinsonian primates showing no inflammatory reaction and strong dopaminergic activity in the left (grafted) putamen compared with the contralateral (ungrafted) hemisphere. (B) Ratio of left (grafted) and right (ungrafted) putaminal Ki values showing the quantification of PET (18F)F-L-DOPA radiotracer at baseline, at MPTP and at 6 mo after grafting in all CTLA4-Ig–grafted (black) and WT-grafted (white) parkinsonian primates of group 2 showing no significant differences in (18F)F-L-DOPA binding over time. (C) Fold increase in locomotor activity from MPTP values quantified at peak recovery (black) and at the last acquired time point (gray) before euthanasia of all primates in group 2, showing a variable degree of improvement over time but no significant difference in locomotor activity improvement between CTLA4-Ig– and WT-grafted primates. (D) Histological analysis of CTLA4-Ig–grafted (top row) and WT-grafted (lower row) primates showing coronal sections at the anterior commissure level stained for TH (I), neurofilament 70 (II), CTLA4-Ig (III), GFAP (IV), Iba1 (V), and CD68 (VI). Data are expressed as mean plus or minus standard error of the mean. Scale bar = 200 μm. (18F)DPA-714, *N,N*-diethyl-2-(2-(4-2-(18F)fluoroethoxy)phenyl)-5,7-dimethylpyrazolo(1,5-a)pyrimidin-3-yl)acetamide; (18F)F-L-DOPA, 6-(18F)fluoro-3,4-dihydroxy-L-phenylalanine; Ki, inhibition constant; MPTP, 1-methyl-4-phenyl-1,2,3,6-tetrahydropyridine; PET, positron emission tomography; mo, months.

parkinsonian primates in group 3 received CTLA4-Ig transgenic porcine neuroblasts under full systemic immunosuppression for 6 mo.

PET was performed with (18F)F-L-DOPA before and after MPTP intoxication and at 6 mo after transplantation (Figures 4AI, II). All primates presented unilateral increases in (18F)F-L-DOPA fixation in the grafted (left) hemisphere compared with the ungrafted hemisphere (Figure 4AII). The mean Ki ratio (left/right) at 6 mo after transplantation (3.66 ± 1.54) was significantly different from the MPTP stage (1.05 ± 0.06) and baseline (1.02 ± 0.02) ($p < 0.01$) (Figure 4B). This correlated with a significant 4.7 ± 0.7-fold improvement of their locomotor activity compared with pretransplantation MPTP values that peaked at day 104 ± 39 ($p < 0.005$). A longitudinal assessment showed that the improvement was long-lasting, with a mean 3.9 ± 0.6-fold increase in motor recovery at 6 mo after grafting compared with MPTP stage ($p < 0.005$) (Figure 4C).

Immunohistochemistry further supported the *in vivo* findings because all grafts stained positively for TH, NF70, CTLA4-Ig and GFAP (Figures 4DI, II, III, IV). A slight positive staining was observed with the neuroinflammation markers Iba1 and CD68 (Figures 4DV, VI).

Animals surviving long term: Two animals from group 3 (6015B and 7774A) were gradually weaned from systemic immunosuppression after 6 mo and followed for 329 and 957 days, respectively.

Longitudinal (18F)F-L-DOPA PET (Figures 5AI, II, III, IV, V) showed a significant increase in amino acid decarboxylase activity in the grafted hemisphere at 6 and 10 mo after transplantation in 6015B and at 10 and 18 mo after transplantation in 7774A, as shown by the increase in the left/right ratio of Ki values over time (Figure 5B, curves). Although later time points showed higher values than MPTP in 7774A, the Ki left/right ratios at 24 and 31 mo were close to 1 because the increase in signal was bilateral (Figures 5AV and B, curves). An (18F)DPA-714 PET scan at the end point showed a unilateral signal on the grafted hemisphere of 7774A that suggested ongoing inflammation 6 mo after the complete withdrawal of all systemic immunosuppression (Figures 5AVI).

Ethovision analysis showed significant recovery in both primates (Figure 5B, histogram). In 6015B, locomotor activity peaked at 3.5 mo (4.3-fold increase) and was 3.5-fold higher than MPTP values at 6 mo after grafting. At 10 mo after grafting, however, the development of a posttransplantation lymphoproliferative disorder caused a reduction in locomotor activity and led to euthanasia. Immunohistochemical analysis revealed very strong staining for TH, NF70, CTLA4-Ig, and GFAP (Figures 5CI–IV) and positive staining for neuroinflammation markers Iba1 and CD68 (Figures 5CV, VI).

Locomotor recovery in 7774A peaked at 3.5 mo after transplantation (6.5-fold increase); fluctuated at 6, 10, 18, and 24 mo after transplantation (3- to 5-fold increase); and reached a sixfold increase at the end point (Figure 5B, histogram). The histological analysis performed at 31 mo after grafting revealed no xenograft and negative staining for TH, NF70 and CTLA4-Ig in the grafted area. A mild astroglial reaction was observed in the targeted left putamen that explained the residual (18F)DPA-714 signal and could represent a signature of an inflammatory process caused by graft rejection (data not shown).

Graft infiltration and expression of IDO

Macroscopically detectable xenografts could be identified in seven of 13 CTLA4-Ig recipients and in only one of six WT recipients.

Immunohistology showed CD3+ T cells, mainly of the CD8+ phenotype, in eight of 13 CTLA4-Ig recipients and in two of six WT recipients (Figures 6A and B). Only two animals grafted with CTLA4-Ig xenografts showed a minority of cells that were positive for both CD3 and Foxp3 (probably CD4+), whereas most cells were CD3+/Foxp3− (probably CD8+; 6895B and 6015B) (Figures 6B and C).

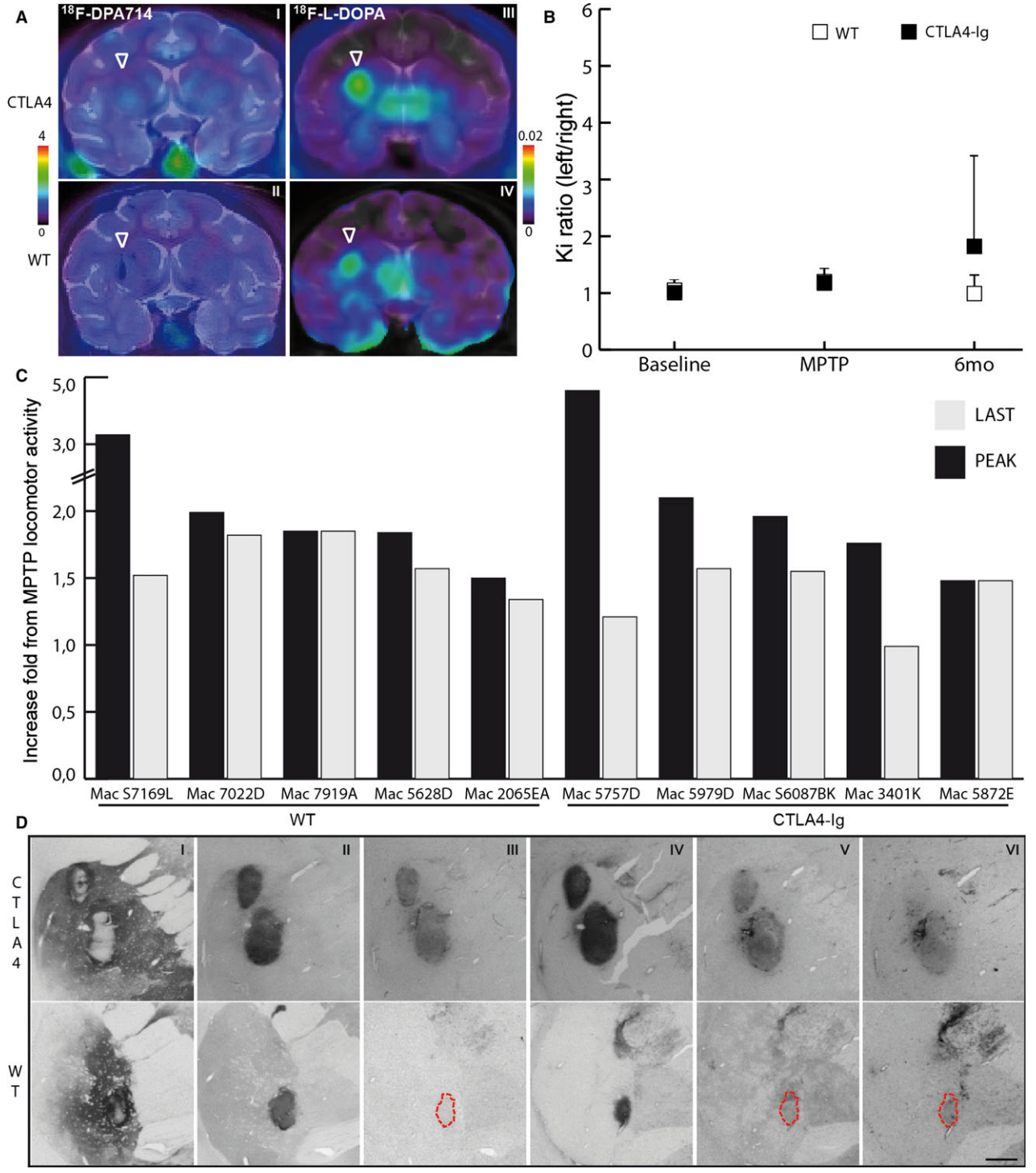

CD20+ B cells coexisted in six of the 10 cases infiltrated with CD3+ cells (Figures 6D and E). In one case (a WT recipient), CD20+ B cells were the only population of lymphocytes observed (data not shown).

The presence of neovessels was consistently associated with infiltration by CD3+ T cells with or without CD20+ B cells, and no cellular infiltration by mononuclear cells was observed in the grafts lacking neovessels (not shown).

Our analyses suggest that CD80 is expressed on Iba1+ microglial cells in both WT and CTLA4-Ig recipients (Figures 6F and G). Interestingly, IDO was observed exclu-

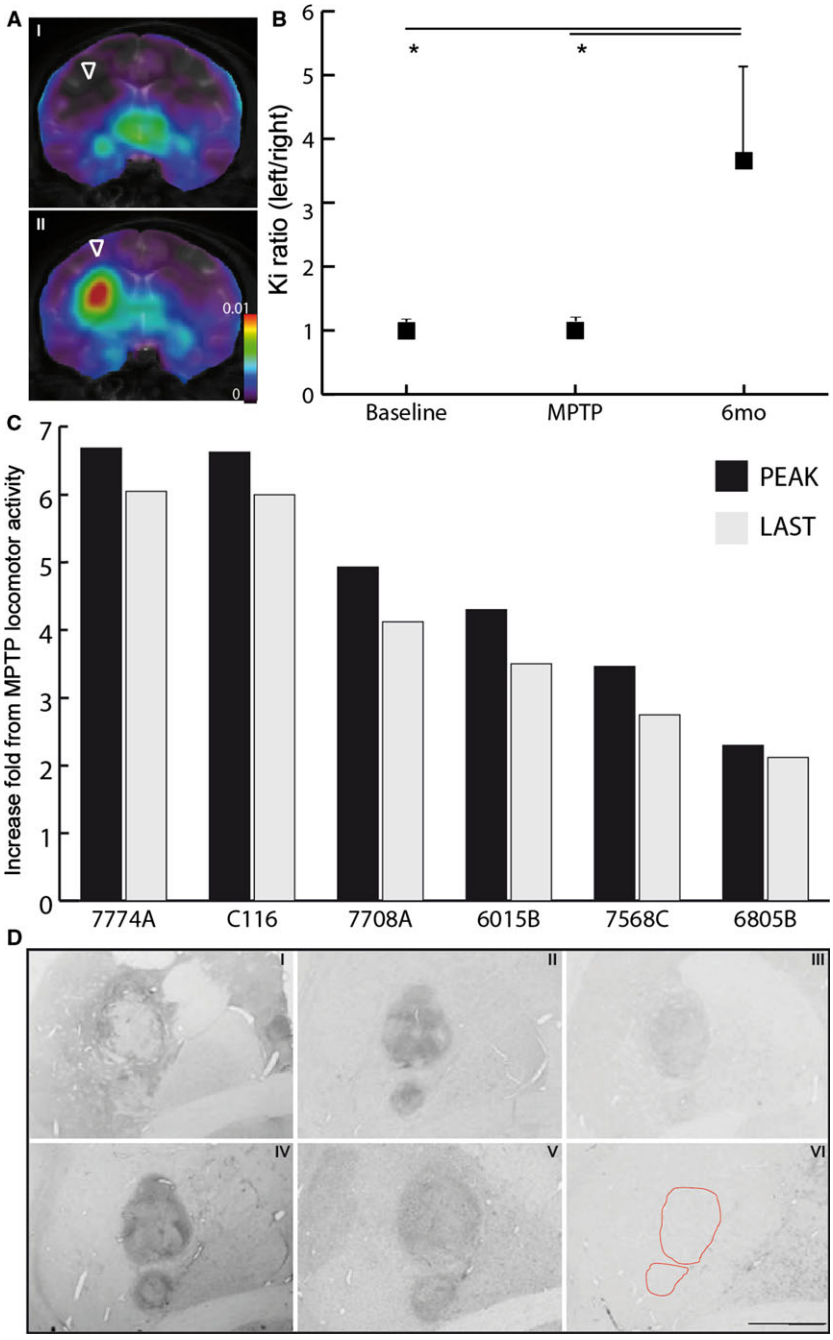

Figure 4: Effect of 6 mo of full peripheral immunosuppressive therapy following CTLA4-Ig porcine embryonic grafts in parkinsonian primates. (A) Representative (18F)F-L-DOPA Ki PET coronal images overlapped with anatomical magnetic resonance imaging at MPTP stage (I) and 6 mo after unilateral transplantation of CTLA4-Ig embryonic cells (II) in a parkinsonian primate showing strong dopaminergic activity in the left (grafted) putamen compared with the contralateral (ungrafted) hemisphere. (B) Ratio of left (grafted) and right (ungrafted) putaminal Ki values showing the quantification of PET (18F)F-L-DOPA radiotracer at baseline, at MPTP and at 6 mo after grafting in all primates in group 3. (C) Fold increase in locomotor activity from MPTP values quantified at peak recovery (black) and at the last acquired time point (gray) before euthanasia in all primates in group 3. (D) Histological analysis of a representative CTLA4-Ig–grafted primate showing coronal sections at the anterior commissure level stained for TH (I), neurofilament 70 (II), CTLA4-Ig (III), GFAP (IV), Iba1 (V), and CD68 (VI). Data are expressed as mean plus or minus standard error of the mean. *$p < 0.01$. Scale bar = 300 μm. (18F)DPA-714, *N,N*-diethyl-2-(2-(4-2-(18F)fluoroethoxy)phenyl)-5,7-dimethylpyrazolo(1,5-a)pyrimidin-3-yl)acetamide; (18F)F-L-DOPA, 6-(18F)fluoro-3,4-dihydroxy-L-phenylalanine; Ki, inhibition constant; MPTP, 1-methyl-4-phenyl-1,2,3,6-tetrahydropyridine; PET, positron emission tomography; mo, months.

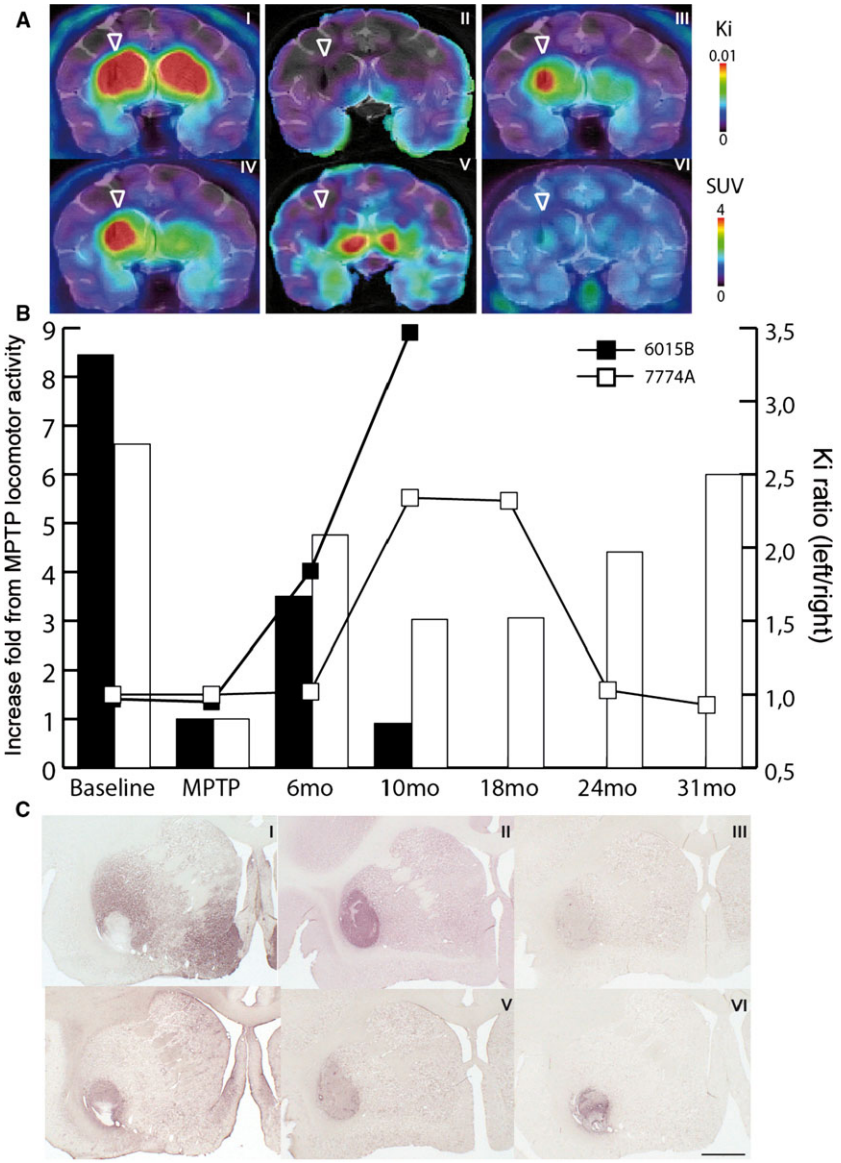

Figure 5: Effect of 6 mo of full systemic immunosuppressive therapy following porcine CTLA4-Ig embryonic cell grafts in parkinsonian primates. (A) Representative (18F)F-L-DOPA Ki PET coronal images overlapped to anatomical MRI images at baseline (I); after MPTP (II); and at 10 mo (III), 18 mo (IV), and 31 mo (V) after unilateral transplantation of CTLA4-Ig cells in primate 7774A, showing strong dopaminergic activity in the grafted putamen at 10 and 18 mo that is lost at 31 mo. (18F)DPA-714 SUV PET coronal images overlapped with anatomical MRI images (VI) showing an inflammatory reaction in the grafted putamen compared with the contralateral (ungrafted) hemisphere at 31 mo after grafting. Imaging results suggest that a dopaminergic graft was present up to 18 mo after transplantation and was rejected thereafter. (B, curves) Ratio of left (grafted) and right (ungrafted) putaminal Ki values showing the quantification of PET (18F)F-L-DOPA radiotracer at baseline, at MPTP, and at several time points after transplantation of CTLA4-Ig pig cells in primates 6015B (black) and 7774A (white), showing the presence of a dopaminergic graft at 10 and 18 mo after transplantation, respectively. (B, bars) Fold increase in locomotor activity from MPTP values quantified at baseline, at MPTP, and at several time points after transplantation in primates 6015B (black) and 7774A (white). (C) Histological analysis of primate 6015B showing coronal sections at the precommissural level stained for TH (I), NF70 (II), CTLA4-Ig (III), GFAP (IV), Iba1 (V), and CD68 (VI). Postmortem results indicated that a surviving (^{18}F)F-L-DOPA PET-positive graft expressed TH as well as CTLA-Ig and NF70 markers. Scale bar = 500 μm. (18F)DPA-714, *N,N*-diethyl-2-(2-(4-2-(18F)fluoroethoxy)phenyl)-5,7-dimethylpyrazolo(1,5-a)pyrimidin-3-yl)acetamide; (18F)F-L-DOPA, 6-(18F)fluoro-3,4-dihydroxy-L-phenylalanine; Ki, inhibition constant; MPTP, 1-methyl-4-phenyl-1,2,3,6-tetrahydropyridine; MRI, magnetic resonance imaging; NF70, neurofilament 70; PET, positron emission tomography; mo, months.

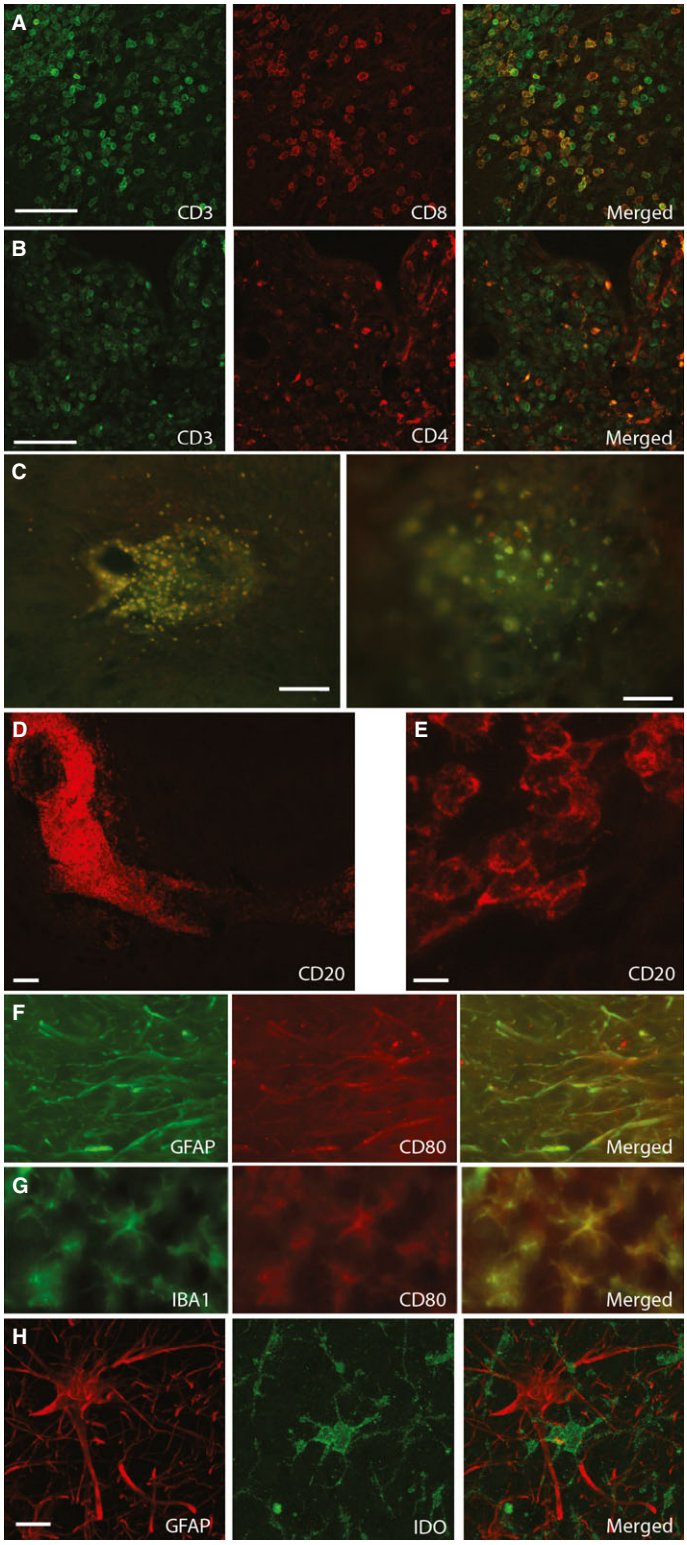

Figure 6: Representative immunohistochemistry of immune cells in recipients of CTLA4-Ig neuroblasts. Animal 6015B (A–E, G, and H) and 6805B (F) showed the presence of T cells (CD3/CD8) (A), CD3/CD4 (B), regulatory T cells (CD3 [green] and Foxp3 [red]) (C), B cells (CD20) (D and E), GFAP/CD80 (F), IBA1/CD80 (G), and GFAP/IDO (H). Scale bars = 100 μm (B, C, and D), 50 μm (A and C), 25 μm (F and G), and 10 μm (E and H).

sively in the seven recipients of CTLA4-Ig xenografts and not in the five WT recipients studied. IDO+ cells were located inside and around the graft. No antibody combination currently allows colabeling with Iba1 to directly associate IDO expression with a microglial marker, and in such an inflammatory context, IDO could also be expressed by mesenchymal or antigen presenting cells. The morphology of the IDO+ cells, however, closely resembles that of microglial cells, and the GFAP staining excludes their astrocytic origin (Figure 6H).

Antipig antibody response following xenotransplantation of neural porcine xenografts

Antipig antibodies were evaluated in the sera of all xenograft recipients using pig aortic endothelial cells as targets. Our data demonstrate that, under systemic immunosuppressive treatment, intracerebral porcine neural xenografts do not elicit a humoral antipig immune response (Figure 7). Indeed, only one animal in group 1 (6788D) that received WT neuroblasts developed a considerable antipig antibody response, detected 1.5 mo after transplantation, 12 days after complete discontinuation of the systemic immunosuppressive therapy; however, low levels of natural antipig antibodies remained stable and detectable in all animals throughout the postoperative period. Furthermore, we confirmed the absence of preexisting or *de novo* antipig antibodies in the CSF (data not shown). Finally, we assessed the presence of antipig donor neuroblast antibodies in the serum of 10 recipients of CTLA4-Ig embryos and three recipients of WT embryos and found them to be negative (data not shown).

Discussion

The translation of novel cell replacement therapy strategies to the clinic is an attractive approach for neurodegenerative disorders (33,34). Treatments currently available to PD patients include deep brain stimulation or pharmacotherapy and gene therapy to replace dopamine. Although very effective in providing transient symptomatic relief, the main limitation of these approaches is that they all require healthy host cells to succeed. In contrast, cell transplantation provides the brain with sustainable benefit because grafted cells can innervate and reconnect the striatum with pertinent brain regions to restore circuitry. In fact, several research consortiums are currently attempting to push embryonic or pluripotent stem cells to the clinic (35–40). In PD, transplantation of allogeneic cells of various origins has led to disparate results including both short-term mild benefit and long-term excellent clinical improvement (7,8). The heterogeneity in the results was explained by differences in the efficacy readouts, injection sites, cell types and numbers, and the degree of differentiation and survival of the implanted cells (1). The preclinical and clinical literature shows that the long-term survival of allogeneic (6, 7, 41–44) and xenogeneic (17,18,45,46) grafts can also be influenced by the presence, type and duration of systemic immunosuppressive therapy. The presence of the blood–brain barrier, the lack of expression of MHC antigens by parenchymal cells or the anti-inflammatory properties of the central nervous system milieu have historically positioned the brain as an immune-privileged site; however, it is now unquestionable that this immune privilege is only partial and may be overcome (47). Consequently, immunosuppression may become a central issue in the design of clinical neural transplantation trials (48,49).

In rodents, the combination of systemic and local immunosuppression has been shown to optimize xenograft survival (50,51). Moreover, the intracerebral administration of a recombinant adenovirus locally overexpressing CTLA4-Ig suppressed both the cellular and humoral immune

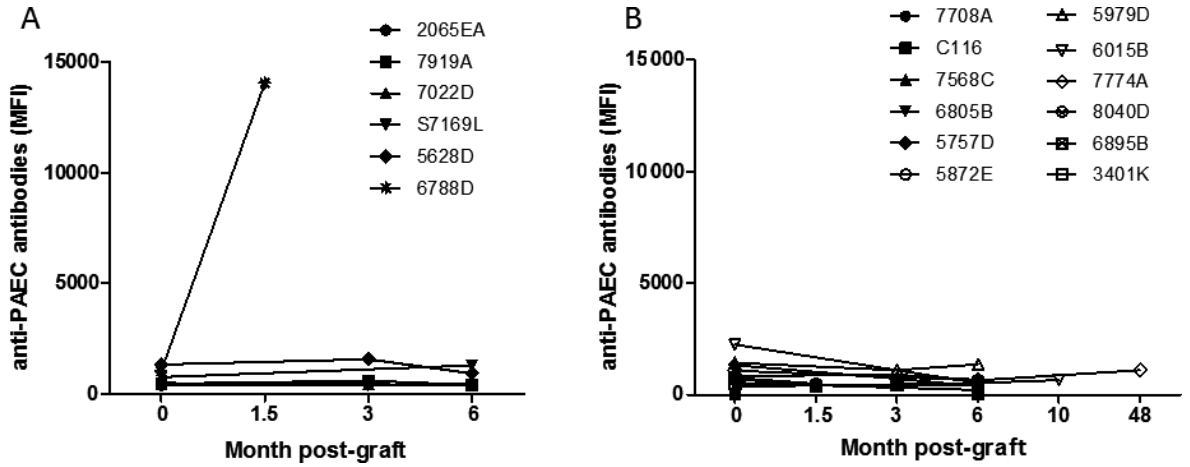

Figure 7: Measurement of antipig antibodies present in the sera of monkeys grafted with WT (A) or CTLA4-Ig (B) ventral mesencephalic pig cells. Cultivated PAEC (A and B) were incubated with sera from nonhuman primates collected at different time points and analyzed by flow cytometry. MFI, median fluorescence intensity; PAEC, porcine aortic endothelial cells.

responses (52,53), suggesting that local CTLA4-Ig expression could contribute to the control of neural xenograft rejection. In this light, a transgenic pig line was developed in which fetal mesencephalic neurons express CTLA4-Ig under the transcriptional control of the neuron-specific enolase promoter (24). Transgenic neural precursors were transplanted into three groups of parkinsonian primates under different durations of peripheral immunosuppressive therapy.

Our studies suggest that expression of CTLA4-Ig by implanted neuroblasts as a stand-alone immunosuppressant is insufficient to protect the xenograft. One month of systemic immunosuppression (meant to cover the initial implantation and differentiation phase) is incapable of preventing rejection; however, we cannot rule out that CTLA4-Ig may have some beneficial immunomodulatory effects that could explain the absence of an important humoral antipig antibody response in the two CTLA4-Ig recipients after withdrawal of systemic immunosuppression that was observed only in the WT recipient from group 1.

Increasing the full immunosuppressive therapy to 3 mo yielded a moderate beneficial effect on locomotion that was associated with a modestly positive (18F)F-L-DOPA signal at 6 mo in some recipients regardless of the type of embryonic cells transplanted; however, the overall effect on locomotor activity progressively reduced as systemic immunosuppressive therapy was gradually withdrawn. This result correlated with the undetectable metabolic activity evaluated by PET at the end point and was further confirmed by the absence of porcine grafts at necropsy. Nonetheless, it is remarkable that in at least three cases, locomotor improvement was maintained despite the loss of grafted cells. This result is in line with numerous publications showing that the endogenous neurotransmitter systems can benefit from neural cell transplantation and gene therapy through mechanisms that include neural protection and trophic factor delivery (54). Such poor graft survival, however, does not allow definitive conclusions about the local immunomodulatory effect of CTLA4-Ig in this group.

When full systemic immunosuppressive therapy was extended to 6 mo, all CTLA4-Ig grafts survived, matured, differentiated and expressed the transgene. This correlated with significant motor recovery and a positive (18F) F-L-DOPA signal on PET. This level of spontaneous recovery was not observed in the severe MPTP model used in this study, as shown in ungrafted controls (Table S3) and in previously published data (55,56). Moreover, the beneficial functional effect could be maintained for several months, even after complete withdrawal of peripheral immunosuppression in the two long-term survivors, which suggests that the recipients were benefiting from the local expression of CTLA4-Ig. (18F)F-L-DOPA PET scans confirmed that the graft was still present and active for up to 18 mo in animal 7774A; however, between years 2 and 3 after transplantation, the (18F)F-L-DOPA signal was reduced in the grafted hemisphere and reached an equivalent level bilaterally. Interestingly, PET with (18F)DPA-714 at the end point indicated an ongoing inflammatory process in the same area, suggesting rejection, and the absence of the porcine xenograft was confirmed at postmortem analysis.

Our hypothesis is that graft rejection is probably caused by peripheral and local presentation of xenoantigens to reactive T cells. Under inflammatory conditions, T cell receptors and costimulatory molecules unaffected by expression of the transgene (e.g. CD154) can be activated by microglial cells through the expression of their ligands (57). Unlike astroglial cells, which can present antigens only during severe neuroinflammation (58), microglial cells can act locally by capturing and presenting xenoantigenic peptides (59–61) and can either migrate to the cervical lymph nodes (13) or promote local amplification of T cells that then patrol the brain (62) or are recruited from the blood through the action of specific chemoattractants. A significant number of CD68+ cells were found within the graft, presumably representing infiltrating macrophages. It is possible that in our experiments, innate immune cells directly recognized and damaged xenogeneic cells, triggering the loss of xenografts independent of an acquired immune response (63). In fact, xenografts did not elicit xenogeneic antibodies in most recipients, suggesting no or little contribution of antigraft antibodies in the rejection process. The observation that expression of CTLA4-Ig was insufficient to inhibit graft rejection might be explained by insufficient levels of CTLA4-Ig or by the elusion of local costimulation blockade by the rejection process. The latter possibility is strongly supported by the observation that most infiltrating CD3+ T cells were CD8+, a phenotype that is CD28− in 50% of cases, and presumably unaffected by the blockade of CD80/86 ligands achieved with CTLA4-Ig. The recent evidence that local expression of CTLA4-Ig on its own is unable to prevent allograft rejection in humanized mice provides additional support for our findings (64).

We further investigated whether the upregulation of IDO was present in the xenografts as the expected biological signature of the action of CTLA4-Ig on CD80-positive antigen presenting cells including microglial cells. We found no expression of IDO in WT xenograft recipients, whereas it was detected most probably in microglial cells in six of 13 CTLA4-Ig xenograft recipients. This observation strongly indicates that CTLA4-Ig expression *in situ* reached a biologically relevant level in our primates. In IDO-expressing grafts presenting neovessels, infiltrating T cells were visible and were not associated with ongoing rejection. These could be either effector cells inhibited by IDO or regulatory T cells supporting immunomodulation by IDO (65). IDO expression in the brain has also been associated with neural protection in experimental autoimmune encephalomyelitis (66). This protective effect, however, is a double-edged sword

because IDO induction can trigger the production of neurotoxic metabolites of the kynurenine pathway, like quinolinic acid (66). In summary, CTLA4-Ig could either block CD80/86-mediated costimulation locally and directly dampen CD28-mediated T cell activation or could indirectly inhibit T cells by eliciting IDO and kynurenine synthesis, preventing potential T cell activation, which might also eventually show neurotoxicity.

In conclusion, we clearly demonstrated that, at least in this species, a combination of local and systemic immunosuppression is needed to sustain the life of a neural cell graft and that CTLA4-Ig alone cannot prevent graft rejection. We validated a translational follow-up approach that combines behavioral, imaging and biomarker screening methodologies to assess the efficacy of a local immunosuppressive strategy for xenotransplantation of porcine fetal ventral mesencephalic neuroblasts in parkinsonian nonhuman primates. This approach allowed us to better monitor the cellular grafts and adapt the immunosuppressive therapy, thus enabling us to achieve the best results to date in terms of graft survival and functional activity in a pig-to-primate xenotransplantation model. Furthermore, we monitored important clinical parameters, like the presence of donor-specific antibodies in this PD xenotransplantation model, which may be critical in facilitating a good graft outcome. This could prove to be highly relevant because the *de novo* appearance of donor-specific antibodies following fetal striatal allo- and xenotransplantation (17) has been reported in recipients with PD and Huntington's disease (6,43,44), with unclear implications for clinical outcome. It is only by associating these fundamental approaches that we will be able to more efficiently translate new cell-based therapies to patients with degenerative neurological diseases.

Acknowledgments

The authors would like to thank Daniele Ramon and Andrea Barzon, whose invaluable contribution and support made this study possible. This work was supported by CORIT (Consortium for Research in Organ Transplantation, Padua, Italy), by the Veneto Region and by the European Commission's Sixth Framework Program, under the priority thematic area Life Sciences, Genomics and Biotechnology for Health, contract N°. LSHB- CT- 2006- 037377, XENOME.

Disclosure

The authors of this manuscript have no conflicts of interest to disclose as described by the *American Journal of Transplantation*.

References

1. Barker RA, Barrett J, Mason SL, Bjorklund A. Fetal dopaminergic transplantation trials and the future of neural grafting in Parkinson's disease. Lancet Neurol 2013; 12: 84–91.
2. Lindvall O. Developing dopaminergic cell therapy for Parkinson's disease–give up or move forward? Mov Disord 2013; 28: 268–273.
3. Brundin P, Kordower JH. Neuropathology in transplants in Parkinson's disease: Implications for disease pathogenesis and the future of cell therapy. Prog Brain Res 2012; 200: 221–241.
4. Brundin P, Li JY, Holton JL, Lindvall O, Revesz T. Research in motion: The enigma of Parkinson's disease pathology spread. Nat Rev Neurosci 2008; 9: 741–745.
5. Cicchetti F, Saporta S, Hauser RA, et al. Neural transplants in patients with Huntington's disease undergo disease-like neuronal degeneration. Proc Natl Acad Sci U S A 2009; 106: 12483–12488.
6. Krystkowiak P, Gaura V, Labalette M, et al. Alloimmunisation to donor antigens and immune rejection following foetal neural grafts to the brain in patients with Huntington's disease. PLoS ONE 2007; 2: e166.
7. Mendez I, Vinuela A, Astradsson A, et al. Dopamine neurons implanted into people with Parkinson's disease survive without pathology for 14 years. Nat Med 2008; 14: 507–509.
8. Kefalopoulou Z, Politis M, Piccini P, et al. Long-term clinical outcome of fetal cell transplantation for Parkinson disease: Two case reports. JAMA Neurol 2014; 71: 83–87.
9. Olanow CW, Gracies JM, Goetz CG, et al. Clinical pattern and risk factors for dyskinesias following fetal nigral transplantation in Parkinson's disease: A double blind video-based analysis. Mov Disord 2009; 24: 336–343.
10. Hagell P, Piccini P, Bjorklund A, et al. Dyskinesias following neural transplantation in Parkinson's disease. Nat Neurosci 2002; 5: 627–628.
11. Drouin-Ouellet J, Barker RA. The challenges of administering cell-based therapies to patients with Parkinson's disease. Neuroreport 2013; 24: 1000–1004.
12. Mathieux E, Nerriere-Daguin V, Leveque X, et al. IgG response to intracerebral xenotransplantation: Specificity and role in the rejection of porcine neurons. Am J Transplant 2014; 14: 1109–1119.
13. Melchior B, Remy S, Nerriere-Daguin V, Heslan JM, Soulillou JP, Brachet P. Temporal analysis of cytokine gene expression during infiltration of porcine neuronal grafts implanted into the rat brain. J Neurosci Res 2002; 68: 284–292.
14. Larsson LC, Frielingsdorf H, Mirza B, et al. Porcine neural xenografts in rats and mice: Donor tissue development and characteristics of rejection. Exp Neurol 2001; 172: 100–114.
15. Barker RA, Ratcliffe E, McLaughlin M, Richards A, Dunnett SB. A role for complement in the rejection of porcine ventral mesencephalic xenografts in a rat model of Parkinson's disease. J Neurosci 2000; 20: 3415–3424.
16. Jacoby DB, Lindberg C, Ratliff J, et al. Fetal pig neural cells as a restorative therapy for neurodegenerative disease. Artif Organs 1997; 21: 1192–1198.
17. Cicchetti F, Fodor W, Deacon TW, et al. Immune parameters relevant to neural xenograft survival in the primate brain. Xenotransplantation 2003; 10: 41–49.
18. Deacon T, Schumacher J, Dinsmore J, et al. Histological evidence of fetal pig neural cell survival after transplantation into a patient with Parkinson's disease. Nat Med 1997; 3: 350–353.
19. Harrower TP, Tyers P, Hooks Y, Barker RA. Long-term survival and integration of porcine expanded neural precursor cell grafts in a rat model of Parkinson's disease. Exp Neurol 2006; 197: 56–69.
20. Honey CR, Charlton HM, Wood KJ. Rat brain xenografts reverse hypogonadism in mice immunosuppressed with anti-CD4 monoclonal antibody. Exp Brain Res 1991; 85: 149–152.

21. Okura Y, Tanaka R, Ono K, Yoshida S, Tanuma N, Matsumoto Y. Treatment of rat hemiparkinson model with xenogeneic neural transplantation: Tolerance induction by anti-T-cell antibodies. J Neurosci Res 1997; 48: 385–396.
22. Wood MJ, Sloan DJ, Wood KJ, Charlton HM. Indefinite survival of neural xenografts induced with anti-CD4 monoclonal antibodies. Neuroscience 1996; 70: 775–789.
23. Poirier N, Blancho G, Vanhove B. A more selective costimulatory blockade of the CD28-B7 pathway. Transpl Int 2010; 24: 2–11.
24. Martin C, Plat M, Nerriere-Daguin V, et al. Transgenic expression of CTLA4-Ig by fetal pig neurons for xenotransplantation. Transgenic Res 2005; 14: 373–384.
25. Menoret S, Plat M, Blancho G, et al. Characterization of human CD55 and CD59 transgenic pigs and kidney xenotransplantation in the pig-to-baboon combination. Transplantation 2004; 77: 1468–1471.
26. Pursel VG, Bolt DJ, Miller KF, et al. Expression and performance in transgenic pigs. J Reprod Fertil Suppl 1990; 40: 235–245.
27. Aron Badin R, Spinnewyn B, Gaillard MC, et al. IRC-082451, a novel multitargeting molecule, reduces L-DOPA-induced dyskinesias in MPTP Parkinsonian primates. PLoS ONE 2013; 8: e52680.
28. Walton A, Branham A, Gash DM, Grondin R. Automated video analysis of age-related motor deficits in monkeys using EthoVision. Neurobiol Aging 2006; 27: 1477–1483.
29. Church JS, Martz DG, Cook NJ. The use of digital video recorders (DVRs) for capturing digital video files for use in both The Observer and Ethovision. Behav Res Methods 2006; 38: 434–438.
30. Cozzi E, Vial C, Ostlie D, et al. Maintenance triple immunosuppression with cyclosporin A, mycophenolate sodium and steroids allows prolonged survival of primate recipients of hDAF porcine renal xenografts. Xenotransplantation 2003; 10: 300–310.
31. Lavisse SIK, Jan C, Peyronneau MA, et al. [18F]DPA-714 PET imaging of translocator protein TSPO (18 kDa) in the normal and excitotoxically-lesioned nonhuman primate brain. Eur J Nucl Med Mol Imaging 2015; 42: 478–494.
32. Vabres B, Le Bas Bernardet S, Riochet D, et al. hCTLA4-Ig transgene expression in keratocytes modulates rejection of corneal xenografts in a pig to non-human primate anterior lamellar keratoplasty model. Xenotransplantation 2014; 21: 431–443.
33. Kriks S, Shim JW, Piao J, et al. Dopamine neurons derived from human ES cells efficiently engraft in animal models of Parkinson's disease. Nature 2011; 480: 547–551.
34. Piquet AL, Venkiteswaran K, Marupudi NI, Berk M, Subramanian T. The immunological challenges of cell transplantation for the treatment of Parkinson's disease. Brain Res Bull 2012; 88: 320–331.
35. TRANSEURO. Available from: http://www.transeuro.org.uk/pages/disease.html; http://www.transeuro.org.uk/pages/TRANSEURO_press%20release%202014.pdf.
36. NYSTEM. Available from: http://nystem.com/developing-cures; https://www.mskcc.org/research-areas/programs-centers/new-york-state-stem-cell-science-consortia.
37. NeuroStemcellRepair. Available from: http://www.neurostemcell-repair.org/.
38. RepairHD. Available from: http://www.repair-hd.eu/.
39. NsGene. Available from: https://www.michaeljfox.org/files/accelerate/participants/NSGene.pdf.
40. Tabar V, Studer L. Pluripotent stem cells in regenerative medicine: Challenges and recent progress. Nat Rev Genet 2014; 15: 82–92.
41. Redmond DE Jr, Vinuela A, Kordower JH, Isacson O. Influence of cell preparation and target location on the behavioral recovery after striatal transplantation of fetal dopaminergic neurons in a primate model of Parkinson's disease. Neurobiol Dis 2008; 29: 103–116.
42. Ma Y, Tang C, Chaly T, et al. Dopamine cell implantation in Parkinson's disease: Long-term clinical and (18)F-FDOPA PET outcomes. J Nucl Med 2010; 51: 7–15.
43. Krebs S, Trippel M, Prokop T, et al. Immune response after striatal engraftment of fetal neuronal cells in patients with Huntington's disease: Consequences for cerebral transplantation programs. Clin Exp Neuroimmunol 2011; 2: 25–32.
44. Porfirio B, Paganini M, Mazzanti B, et al. Donor-specific anti-HLA antibodies in Huntington's disease recipients of human fetal striatal grafts. Cell Transplant 2015; 24: 811–817.
45. Schumacher JM, Ellias SA, Palmer EP, et al. Transplantation of embryonic porcine mesencephalic tissue in patients with PD. Neurology 2000; 54: 1042–1050.
46. Lee SR, Lee HJ, Cha SH, et al. Long-term survival and differentiation ofhuman neural stem cells in nonhuman primate brain with no immunosuppression. Cell Transplant 2015; 24: 191–201.
47. Galea I, Bechmann I, Perry VH. What is immune privilege (not)? Trends Immunol 2007; 28: 12–18.
48. Lindvall O, Bjorklund A. Cell therapy in Parkinson's disease. NeuroRx 2004; 1: 382–393.
49. Olanow CW, Goetz CG, Kordower JH, et al. A double-blind controlled trial of bilateral fetal nigral transplantation in Parkinson's disease. Ann Neurol 2003; 54: 403–414.
50. Leveque X, Cozzi E, Naveilhan P, Neveu I. Intracerebral xenotransplantation: Recent findings and perspectives for local immunosuppression. Curr Opin Organ Transplant 2011; 16: 190–194.
51. Leveque X, Mathieux E, Nerriere-Daguin V, et al. Local control of the host immune response performed with mesenchymal stem cells: Perspectives for functional intracerebral xenotransplantation. J Cell Mol Med 2015; 19: 124–134.
52. Ideguchi M, Kajiwara K, Yoshikawa K, Uchida T, Ito H. Local adenovirus-mediated CTLA4-immunoglobulin expression suppresses the immune responses to adenovirus vectors in the brain. Neuroscience 2000; 95: 217–226.
53. Uchida T, Kajiwara K, Ideguchi M, Yoshikawa K, Morioka J, Suzuki M. Co-administration of adenovirus vector expressing CTLA4-Ig prolongs transgene expression in the brain of mice sensitized with adenovirus. Brain Res 2001; 898: 272–280.
54. Xu H, Belkacemi L, Jog M, Parrent A, Hebb MO. Neurotrophic factor expression in expandable cell populations from brain samples in living patients with Parkinson's disease. FASEB J 2013; 27: 4157–4168.
55. Kishima H, Poyot T, Bloch J, et al. Encapsulated GDNF-producing C2C12 cells for Parkinson's disease: A pre-clinical study in chronic MPTP-treated baboons. Neurobiol Dis 2004; 16: 428–439.
56. Jarraya B, Boulet S, Ralph GS, et al. Dopamine gene therapy for Parkinson's disease in a nonhuman primate without associated dyskinesia. Sci Transl Med 2009; 1: 2ra4.
57. Olson JK, Miller SD. Microglia initiate central nervous system innate and adaptive immune responses through multiple TLRs. J Immunol 2004; 173: 3916–3924.
58. Gimsa U, Mitchison NA, Brunner-Weinzierl MC. Immune privilege as an intrinsic CNS property: Astrocytes protect the CNS against T-cell-mediated neuroinflammation. Mediators Inflamm 2013; 2013: 320519.
59. Poltorak M, Freed WJ. Immunological reactions induced by intracerebral transplantation: Evidence that host microglia but

not astroglia are the antigen-presenting cells. Exp Neurol 1989; 103: 222–233.
60. Shinoda M, Hudson JL, Stromberg I, Hoffer BJ, Moorhead JW, Olson L. Microglial cell responses to fetal ventral mesencephalic tissue grafting and to active and adoptive immunizations. Exp Neurol 1996; 141: 173–180.
61. Hickey WF, Kimura H. Perivascular microglial cells of the CNS are bone marrow-derived and present antigen *in vivo*. Science 1988; 239: 290–292.
62. Wekerle H, Sun D, Oropeza-Wekerle RL, Meyermann R. Immune reactivity in the nervous system: Modulation of T-lymphocyte activation by glial cells. J Exp Biol 1987; 132: 43–57.
63. Wang H, Yang YG. Innate cellular immunity and xenotransplantation. Curr Opin Organ Transplant 2012; 17: 162–167.
64. Rong Z, Wang M, Hu Z, et al. An effective approach to prevent immune rejection of human ESC-derived allografts. Cell Stem Cell 2014; 14: 121–130.
65. Sucher R, Fischler K, Oberhuber R, et al. IDO and regulatory T cell support are critical for cytotoxic T lymphocyte-associated Ag-4 Ig-mediated long-term solid organ allograft survival. J Immunol 2012; 188: 37–46.
66. Kwidzinski E, Bechmann I. IDO expression in the brain: A double-edged sword. J Mol Med (Berl) 2007; 85: 1351–1359.

Supporting Information

Additional Supporting Information may be found in the online version of this article.

Data S1: Supplemental Material and Methods.

Table S1: List of experimental groups.

Table S2: Summary of the systemic immunosuppressive therapy.

Table S3: Longitudinal locomotor activity data in ungrafted parkinsonian primates.

Figure S1: Assessment of dopaminergic depletion in the MPTP model of Parkinson's disease in nonhuman primates. (A) Ki values showing the quantification of PET (18F)F-L-DOPA radiotracer in the left (black) and right (white) putamen compared with the occipital cortex at control and MPTP stages for all primates subdivided into future treatment groups, showing a significant bilateral reduction in tracer uptake after MPTP intoxication. (B) (18F)F-L-DOPA Ki PET representative coronal images overlapped with anatomical magnetic resonance imaging at baseline (I) and MPTP stages (II) showing dopaminergic depletion in the striatum (C). Ethovision analysis of the total distance moved in 40 min of film at control (black) and MPTP (gray) stages for all primates subdivided into their future treatment groups. Data are expressed as a percentage of locomotor activity measured at baseline for each subject and shows severe reduction in locomotor activity after MPTP intoxication. (D) Representative Ethovision tracking maps illustrating the trajectory (red lines) and amount of movement (density of lines) quantified in 40-min films before (I) and after MPTP intoxication (II). (E) Histograms displaying a significant reduction in the number of TH+ neurons in the SNpc following postmortem stereological cell counts in parkinsonian (gray) primates compared with intact (black) controls. (F) Representative coronal sections (40 μm) stained with TH showing the loss of dopaminergic terminals in the striatum (I and II) and cell bodies in the SNpc (III and IV) in parkinsonian primates compared with intact controls. Data are expressed as mean plus or minus standard error of the mean. $^{**}p < 0.001$. Scale bars = 500 μm. Ki, inhibition constant; MPTP, 1-methyl-4-phenyl-1,2,3,6-tetrahydropyridine; SNpc, substantia nigra pars compacta.